Opto-Electronics Review

journal homepage: https://journals.pan.pl/opelre

Dynamic coordination of photovoltaic-storage-charging in transportation service areas considering photovoltaic fluctuation

Lei Zhang, Lipeng Cao, Wenyong Yang, Yang Yu, Yuanxuan Pan*

Research Institute of Digital & Intelligent Transportation, Hubei Communications Planning and Design Institute Co., Ltd., Wuhan, China

Article info

Article history:
Received 28 Feb. 2026
Received in revised form 29 Apr. 2026
Accepted 05 May 2026
Available on-line 21 Jul. 2026

Keywords:
photovoltaic fluctuation;
energy storage characteristics;
charging load characteristics;
uncertainty set of fluctuation;
transportation service area;
dynamic coordinated dispatch.

Abstract

This article proposes a dynamic coordination and scheduling method for photovoltaic, energy storage, and charging systems in highway service areas. Based on the topology of the DC distribution network in the service area, we analyse the dynamic characteristics of each element, characterise the photovoltaic stochastic process using beta distribution and construct a multi-objective model. The objectives include maximising photovoltaic integration, minimising output tracking deviation and system operating costs, and maximising energy storage revenue, as well as integrating photovoltaic output, energy storage state of charge, and charging load fluctuations into an uncertainty set, embedding robust constraints to enhance anti-interference, and combining fuzzy membership functions with an improved whale optimisation algorithm to achieve multi-objective optimisation. Simulation results show that this method effectively smooths the peak to valley load, reducing the peak load to below 300 kW and reducing the peak to valley difference to 200 kW. Under various fluctuation scenarios, the photovoltaic utilization rate exceeds 90%, energy storage output is safe, and user comfort loss remains stable between 0.102 and 0.113. This study provides a dynamic scheduling solution for energy systems in the field of transportation services, balancing renewable energy integration, economic efficiency, safety, and user experience.

1. Introduction

The transportation service area is the core scenario for electric vehicle charging, with abundant spatial resources such as roofs and parking lot canopies, etc., which are conducive to the construction of distributed photovoltaic power generation systems and the formation of an integrated photovoltaic charging mode with self-generated electricity for self-use and surplus electricity connected to the grid. It is an effective way to achieve low-carbon, sustainable development in transportation energy. However, photovoltaic power generation is affected by factors such as weather, solar intensity, and cloud movement [1], making it highly random and uncertain. If directly coupled with randomly arriving electric vehicle charging loads, this will cause significant surges in the distribution network in the service area [2]. At the same time, the charging load of electric vehicles is uncertain in both time and space, and the demand for "tidal" charging during holidays differs significantly from that during non-peak hours in daily life. The interaction mechanism between traditional power grids and distributed energy is not yet mature, and the tension between limited distribution capacity in service areas and the surge in charging demand is pronounced, leading to reduced solar power generation [3] and higher electricity costs. Integrating energy storage systems to form a photovoltaic energy storage and charging microgrid is an ideal solution for reducing photovoltaic fluctuations, improving energy efficiency and economy. However, existing energy storage charging and discharging strategies lack dynamic adaptability, and fixed thresholds cannot address the dual uncertainties of photovoltaic fluctuations and charging demand [4]. Moreover, frequent deep charging and discharging can accelerate battery

*Corresponding author at: panyx26@igit.ac.cn

https://doi.org/10.24425/opelre.2026.1615
1896-3757/ Association of Polish Electrical Engineers (SEP) and Polish Academy of Sciences (PAS). Published by PAS

capacity degradation. Therefore, coordinating the scheduling of photovoltaic, energy storage, and charging loads is the core challenge for the safe, stable, and economical operation of distribution networks in service areas [5]. Traditional static or one-day-advance scheduling strategies struggle to handle dual randomness and cannot fully tap into the system potential.

To address related issues, Alamir *et al*. [6] proposed a multi-objective optimisation method for managing renewable energy. This method integrates renewable energy sources, such as solar photovoltaics, with hybrid energy storage systems (HESS) and demand response, and estimates renewable energy production using historical data and meteorological forecasts. Its goal is to reduce the operating and power trading costs of traditional generators, increase operator revenue, and reduce peak loads, using a mixed ε-dictionary-weighted sum method for the solution. This approach still relies on historical data and simple meteorological models (e.g., irradiance, temperature) to forecast renewable energy output, failing to adequately address the dual randomness of PV generation and charging loads, thereby limiting its applicability. Zadehbagheri *et al*. [7] examined photovoltaic power generation and electric vehicle charging/discharging behaviour in hybrid economic emission scheduling from multiple perspectives. While considering economic constraints, they proposed a multi-objective model with dual cost and pollution targets, aiming to reduce economic emissions and efficiently schedule renewable energy. An improved whale optimisation algorithm (WOA) was employed to obtain the optimal solution, yielding the lowest-cost, lowest-emission energy management plan satisfying all constraints. However, during application, the multi-objective optimisation must handle non-linear and non-convex constraints, causing computational complexity to increase exponentially with system scale and making it difficult to meet real-time control requirements. Mobtahej *et al*. [8] proposed a three-stage demand-side management framework: a first-order uncertainty minimisation model; second-order microgrid and integrated demand-side management (DSM) information; third-order model predictive control is used to optimise distributed generation (DG) scheduling, and renewable energy is managed according to actual scheduling. However, demand response strategies (e.g., load interruptions, energy storage charging/discharging) may compromise user comfort or increase equipment wear, leading to low user participation and uncertain management effectiveness. Sreenivasulu *et al*. [9] proposed a coordinated stochastic dispatch model that accounts for uncertainty in renewable energy sources (RES). This incorporates transaction penalty costs and generation rescheduling costs into the dispatch model to reduce generator dispatch transactions and output variations. To more effectively analyse the impact of renewable uncertainty on transaction plan scale, system operators or power traders can implement appropriate measures based on safety and economic conditions to ensure the safe and economical operation of TEMs, achieving trading and optimised scheduling without considering any safety or economic issues. However, when conflicts arise between renewable energy output and market-based economic planning in practice, this method cannot effectively address these scenarios.

Recent studies [10–12] have specifically addressed solar-powered electric vehicle (EV) charging stations, highlighting the need for dynamic coordination to handle photovoltaic intermittency. Based on the above analysis, this paper aims to achieve a dynamic collaborative scheduling of photovoltaic-storage-charging in highway service areas, ensure the effective use of renewable energy, and realise the safe and stable operation of the distribution network in service areas. By analysing the fluctuation characteristics of photovoltaic output in service areas and fully integrating the fluctuation of photovoltaic generation with the characteristics of energy storage, a dynamic collaborative scheduling model for photovoltaic-storage-charging in highway service areas is established. On this basis, the dynamic characteristics of photovoltaic-storage-charging are used to complete collaborative scheduling, providing theoretical foundations and technical support for the construction and operation of green highway service areas [13]. The conceptual novelty of this work is threefold: (i) a unified uncertainty set that jointly models photovoltaic fluctuation, charging load randomness, and energy storage SOC dynamics, enabling coordinated scheduling that accounts for their interdependencies; (ii) integration of fuzzy membership functions with an improved WOA specifically tailored to this tripartite uncertainty framework; (iii) explicit quantification of user comfort loss as an optimisation objective, balancing renewable integration, economic efficiency, and user experience in transportation service areas.

2. Dynamic coordination of photovoltaic-storage-charging in transportation service areas

2.1. Operational characteristics of transportation service area distribution networks considering photovoltaic fluctuation

2.1.1 DC distribution network system topology in transportation service areas

The distribution network in transportation service areas primarily employs DC distribution. Photovoltaic panels are installed on service area rooftops and highway open spaces, connected to the DC busbar via DC conversion. DC charging stations connect to the DC busbar, with energy storage configured according to system requirements. Bidirectional energy storage converters enable connection to the DC busbar. The busbar supplies conventional loads such as lighting, office equipment, and appliances in living areas (low-voltage DC appliances). The topology structure of the DC distribution network system in transportation service areas is shown in Fig. 1.

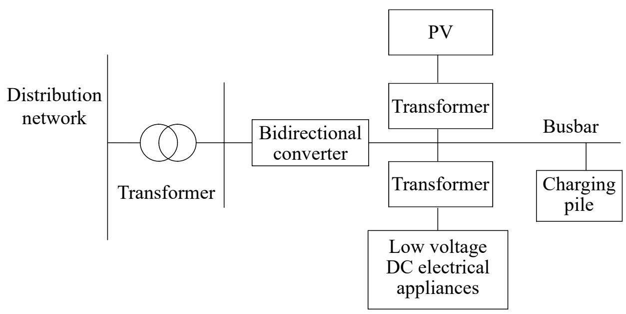

Fig. 1. Topology structure of DC distribution network system in transportation service area.

In the topology of the DC distribution network in the transportation service area, the installation locations of photovoltaic panels can be selected based on local conditions, such as building roofs, square carports, open spaces, and slopes near highways. When selecting the type of photovoltaic array, stability and high efficiency are the primary considerations. The energy storage system is connected to the DC bus through a bidirectional converter, which can smooth the load and provide temporary power at night or when photovoltaic power cannot be generated. The storage capacity can be designed according to goals such as economic feasibility and reliability [14].

According to the topology shown in Fig. 1, in the photovoltaic energy storage and charging coordination scheduling system, energy storage serves as the core intermediary between photovoltaic power generation and charging loads. The key is to store excess energy when photovoltaic capacity exceeds demand and release it when demand is insufficient. Coordinating charging-station demand (including peak-valley characteristics and power requirements) is the foundation for achieving high photovoltaic integration, optimal energy storage utilisation, and high reliability of charging services in the DC distribution network of transportation service areas.

2.1.2 Analysis of photovoltaic fluctuation in DC distribution networks at transportation service areas

The solar irradiance is affected by random factors such as cloud cover, atmospheric scattering, and terrain reflection, leading to significant fluctuations and intermittency, resulting in highly unstable active power output from photovoltaic systems. To describe this behaviour, this article adopts a beta distribution, whose shape parameters α and β can be flexibly adjusted in the distribution form (such as skewness and peak position) to adapt to the actual fluctuation patterns of solar irradiance in different time periods and geographical regions. Therefore, given an approximate beta distribution of solar irradiance within a given interval, the beta distribution formula for photovoltaic output characteristics that fully consider influencing factors is as follows:

$$\rho(F_t)=\frac{\Gamma(\alpha+\beta)}{P_{\max}\times\Gamma(\alpha)\Gamma(\beta)}\cdot\left(\frac{F_t}{F_t^{\max}}\right)^{\alpha-1}\cdot\left(1-\frac{P_t}{P_{\max}}\right)^{\beta-1} \tag{1}$$

$$\begin{cases}\alpha=\mu\cdot\left[\dfrac{\vec{\eta}\cdot(1-\mu)}{\sigma^2}-1\right]\\ \beta=(1-\mu)\cdot\left[\dfrac{\vec{\eta}\cdot(1-\mu)}{\sigma^2}-1\right]\end{cases}. \tag{2}$$

Among them, $\rho(F_t)$ is the probability density when the solar irradiance is F_t, Γ is the Gamma function, $F_t^{\max}$ is the maximum solar irradiance during the statistical period, $P_{\max}$ is the maximum power output of the photovoltaic system, μ and ρ represent the average and standard deviation of irradiance during the statistical period.

Equation (1) gives the probability density function of the output power of the photovoltaic module. Based on this, the photovoltaic active power output P_t at time t using the following formula can be calculated:

$$P_t=P_0\times\frac{F_t}{F_t^{\max}}\chi(R_1-R_2). \tag{3}$$

Among them, P_0 is the rated active power output, χ is the temperature coefficient, and R_1 and R_1, respectively, refer to the temperature of the photovoltaic module and the ambient temperature.

From this, it can be seen that photovoltaic power has non-linear characteristics and varies with changes in influencing factors, resulting in significant fluctuations in photovoltaic output [15].

2.1.3 Analysis of energy storage characteristics in DC distribution networks of transportation service areas

In the DC distribution network of transportation service areas, the energy storage system is a multifunctional stabiliser and energy dispatch centre, playing a multi-dimensional and critical role. In this type of distribution network, fluctuating loads, such as electric vehicle charging stations, coexist with intermittent power sources, such as photovoltaic power generation. When multiple electric vehicles charge simultaneously [16], the sudden increase in electricity demand strains the power grid, and the energy storage system can quickly discharge to fill the gap. When demand for charging decreases, excess power is absorbed, the power curve is smoothed, voltage drops or surges are prevented, and electricity costs in the service area are reduced.

The battery capacity and number of units in the energy storage system are determined by the charging load power demand and the continuous discharge duration. The SOC formula is as follows:

$$S_j^t=\begin{cases}S_j^0, & t=0\\ S_j^{t-1}+\Delta t\times\left(\dfrac{\bar{P}_j\bar{\eta}_j}{E_j^0}-\dfrac{\vec{P}_j}{E_j^0\times\vec{\eta}_j}\right), & 0<t<T\end{cases}. \tag{4}$$

Among them, S_j^t is SOC of the j-th battery at time t, S_j^0 is the initial SOC of the battery, E_j^0 is its rated capacity, $\bar{P}_j$. $\vec{P}_j$ represents the charging and discharging power of the j-th battery, $\bar{\eta}_j$. $\vec{\eta}_j$ represents its charging and discharging efficiency, T represents the cycle, and Δt represents the time interval.

Using the SOC formula, the dynamic variation of energy storage SOC with respect to charging/discharging power, efficiency, and time is clarified. Based on "charging load demand + continuous discharge duration", the energy storage capacity is determined to ensure its regulation capability matches the actual requirements of photovoltaic fluctuations and charging load variations [17], avoiding under-provisioning or redundancy.

2.1.4 Analysis of DC distribution network charging load characteristics in transportation service areas

Let $P_{i,L}^t$ denote the charging power of an individual electric vehicle i at time t. For a given charging node n, the total charging load at that node at time t, denoted $P_{n,L}^t$, is the sum of the charging powers of all EVs connected to node n:

$$\widehat{P}_L^t = \sum_{i=1}^{N_1} P_{n,L}^t, \tag{5}$$

where N_1 denotes the number of electric vehicles charging node at time t.

The total system-wide charging load $P_{n,L}^t$, at time t is then obtained by aggregating the loads across all charging nodes in the distribution network:

$$P_{i,L}^t = \sum_{i=1}^{N_2} \widehat{P}_L^t, \tag{6}$$

where N_2 denotes the number of charging nodes.

Using the above formula, one can calculate the charging load from a single electric vehicle → to a single charging node → to the entire distribution network (from micro to macro), clearly identifying the charging power demand at different times and nodes [18]. This allows for understanding the "spatio-temporal characteristics" of the load (when, where, and how much charging demand exists). Furthermore, by integrating the coupling relationship between transportation nodes and the distribution network, the impact/intermittent nature of the charging load can be analysed.

2.2. *Photovoltaic-storage-charging coordinated dispatch model*

2.2.1 Objective function definition

To achieve dynamic collaborative scheduling of photovoltaic-storage-charging, this paper designs a collaborative scheduling model based on the structural characteristics of the traffic service area. The model is developed from four perspectives: first, ensuring the consumption capacity of photovoltaic power under the premise of accounting for photovoltaic fluctuation; second, controlling the deviation between the actual output of the combined system and the reference value obtained from scheduling within the scheduling cycle; third, controlling the cost of collaborative scheduling; and fourth, considering the revenue result of energy storage entities. Based on this, the model includes four objectives: maximising PV consumption maxf_1, minimising the deviation between the actual combined output of the traffic service area and the reference value obtained from scheduling minf_2, minimising the cost of collaborative scheduling minf_3, and maximising the revenue of energy storage entities minf_4. The calculation formulas for these four objective functions are as follows:

$$\max f_1 = \sum_{t=1}^{T} \sum_{i=1}^{N_3} P_i^t \tag{7}$$

$$\begin{cases} \min f_2 = \dfrac{1}{T} \sum_{t=1}^{T} \left(\vec{P}_\Sigma - \vec{P}_o \right) \\ \vec{P}_\Sigma = P_i^t + \vec{P}_j \end{cases} \tag{8}$$

$$\min f_3 = \sum_{t=1}^{24} \left(C_t^1 + C_t^e + C_t^2 + C_t^a \right) \tag{9}$$

$$\max f_4 = C_e + C_L - C_1 - \sum_{i=1}^{T} C_t^2, \tag{10}$$

where N_3 denotes the number of PV nodes connected to the transportation service area, $\vec{P}_\Sigma$ represents the total power output of the transportation service area, $\vec{P}_o$ indicates the joint power generation plan for the transportation service area, C_L and C_e denote the revenue from energy storage and vehicle charging loads, and distribution network transactions, respectively, C_1 represents the transmission fees paid when energy storage directly sells electricity to charging loads, C_t^2 indicates the maintenance cost of the energy storage system, C_t^1 denotes the PV operation and maintenance cost, C_t^a represents the carbon emission cost.

2.2.2 Constraint design

After constructing the objective function for the photovoltaic-storage-charging coordinated dispatch model as described above, corresponding constraints must be designed to ensure the feasibility of the coordinated dispatch and the practicality of the dispatch results. The equipment-related constraints are outlined below:

(1) Fluctuation uncertainty set constraint:

The objective of "photovoltaic-storage-charging" coordination is to balance the power/energy relationship among photovoltaic (power source), energy storage (regulation), and charging load (demand). Based on the characteristics of photovoltaic systems, energy storage systems, and charging loads analysed in subsections 2.1.2, 2.1.3, and 2.1.4 above: – photovoltaic output is intermittent [19] and random due to sunlight and temperature influences (uncontrollable fluctuations); – charging load is impacted by electric vehicle arrival/charging behaviour, exhibiting impactful, temporally and spatially random characteristics (uncontrollable demand); – although energy storage systems serve as regulation resources, their output is constrained by charging/discharging efficiency and SOC limitations (uncontrollable state), (uncontrollable fluctuations), charging loads exhibit impact-like, spatiotemporally distributed randomness (uncontrollable demand) due to electric vehicle arrival/charging behaviour, and while energy storage systems serve as regulation resources, their actual regulation capacity dynamically fluctuates (boundary-constrained response) due to constraints from charge/discharge efficiency and SOC status. Analysing the uncertainty of any single component individually cannot cover the entire fluctuation risk of the system [20], compromising the comprehensiveness of coordinated scheduling. Therefore, to ensure the effectiveness of dynamic coordinated scheduling for photovoltaic-storage-charging in transportation service areas, this paper integrates the three components into a unified uncertainty set Ω for modelling fluctuation uncertainty. The constructed fluctuation uncertainty set is as follows:

$$\Omega = \left\{ P_t, \widehat{P}_L^t, S_j^t \right\} \tag{11}$$

$$\begin{cases} \begin{Bmatrix} P_t^{\min} \le P_t \le P_t^{\max} \\ \widehat{P}_L^{t,\min} \le \widehat{P}_L^t \le \widehat{P}_L^{t,\max} \\ \vec{P}_j^{t,\min} \le \vec{P}_j^t \le \vec{P}_j^{t,\max} \\ \vec{P}_j^{t,\min} \le \vec{P}_j^t \le \vec{P}_j^{t,\max} \end{Bmatrix}. \\ \sum_{k=1}^{3} \left| \dfrac{b_k^t - \tilde{b}_k^t}{\Delta b_k^{\max}} \right| \le \kappa \end{cases} \tag{12}$$

In the formula, b_k^t is the actual value of an uncertain parameter variable, which includes three variables, namely P_t, $\widehat{P}_L^t$, S_j^t, $k = 1,2,3$, $\tilde{b}_k^t$ represents the predicted value of uncertain parameter variables, $\Delta b_k^{\max}$ represents the maximum deviation between the actual and predicted values of uncertain parameter variables, κ represents the adjustable parameters for uncertain variables. The upper and lower limits of P_t are represented by $P_t^{\max}$ and $P_t^{\min}$. The upper and lower limits of $\widehat{P}_L^t$ are represented by $\widehat{P}_L^{t,\max}$ and $\widehat{P}_L^{t,\min}$, while the upper and lower limits of $\overleftarrow{P}_j^t$ are represented by $\overleftarrow{P}_j^{t,\max}$ and $\overleftarrow{P}_j^{t,\min}$. The upper and lower limits of $\vec{P}_j^t$ are represented by $\vec{P}_j^{t,\max}$ and $\vec{P}_j^{t,\min}$.

Based on the above constraint equations, the uncertainty set for fluctuation is constructed as Ω. Ω unifies the uncertainties of photovoltaic (power source fluctuations), charging load (demand fluctuation), and energy storage SOC (regulation capability fluctuation) into a "computable boundary". This enables dispatch plans to clearly define the required fluctuation range, adapt to dynamic changes in photovoltaic-storage-charging systems, and provide deviation correction references for real-time dispatch. It prevents power imbalances or voltage limit violations caused by overlooking fluctuations in any component [21].

(2) Charging demand and load constraints:

During dynamic photovoltaic-storage-charging coordination, scheduling must adapt to PV fluctuations by adjusting charging loads [22] to reduce costs without compromising users' experience or exceeding equipment capacity. This balances the rigidity and flexibility of charging demands. The constraint formula is:

$$\sum_{t=1}^{T} \widehat{P}_L^t = \sum_{t=1}^{T} \tilde{P}_L^t \tag{13}$$

$$\frac{\sum_{t=1}^{T} \left| \widehat{P}_L^t - \tilde{P}_L^t \right|}{\sum_{t=1}^{T} \widehat{P}_L^t} \le \varphi_{\max}, \tag{14}$$

where $\tilde{P}_L^t$ denotes the charging load after coordinated scheduling, $\varphi_{\max}$ represents the upper limit of the adjustable proportion of electric vehicle charging load.

(3) Equipment output power constraint:

During coordinated scheduling, to ensure reasonable distribution of PV output power and guarantee the safe operation of PV equipment, PV output power constraints are established. The formula is:

$$\begin{cases} \left| Q_i^t \right| \le \sqrt{R_{t,i}^2 - P_{t,i}^2} \\ 0 \le \hat{P}_t \le P_t \\ 0 \le \breve{P}_t \le P_t \\ 0 \le \overline{P}_t \le P_t \end{cases}, \tag{15}$$

where Q_i^t represents the reactive power output from PV at the connection node i, $R_{t,i}$ denotes the PV connection capacity at that node, $\hat{P}_t$, $\breve{P}_t$, and $\overline{P}_t$, respectively, represent the power directly supplied by PV to the energy storage system, the power supplied to the transportation service area distribution network, and the power supplied for electric vehicle charging.

(4) Energy storage device operational constraints:

Under the four-objective framework for dynamic coordination of photovoltaic-storage-charging, the following constraints ensure the energy storage system: – rapid response to PV fluctuations and charging load impacts, – timely mitigation of deviations between actual output and reference values, – avoidance of frequent deep charge/discharge cycles, – ability to absorb surplus PV energy during excess generation (preventing curtailment) while preventing equipment damage from overcharging/ damage equipment due to overcharging/overdischarging, enabling the PV integration target to be achieved within safe limits. The operational constraint formula for the energy storage device is designed as follows:

$$\begin{cases} \overleftarrow{g}_t \overleftarrow{P}_t^{\min} \le \overleftarrow{P}_j^t \le \overleftarrow{g}_t \overleftarrow{P}_t^{\max} \\ \vec{g}_t \vec{P}_t^{\min} \le \vec{P}_j^t \le \vec{g}_t \vec{P}_t^{\max} \\ \overleftarrow{g}_t, \vec{g}_t \in \{0,1\} \\ \overleftarrow{g}_t + \vec{g}_t \le 1 \end{cases}, \tag{16}$$

$$\begin{cases} S_j^{t,\min} \le S_j^t \le S_j^{t,\max} \\ S_j^0 = S_j^z \\ S_j^{t+1} = S_j^t + \Delta S_j^t \\ \Delta S_j^t = \dfrac{\overleftrightarrow{P}_j^{t,\max} \times \Delta t}{E_j^0} \end{cases}, \tag{17}$$

$$E_\Sigma^t = \left(\overleftarrow{P}^t \times \overleftarrow{\eta}_j - \frac{\vec{P}^t}{\vec{\eta}_j} \right) \Delta t + E_\Sigma^{t-1}, \tag{18}$$

$$\begin{cases} E^{\min} \le E^t \le E^{\max} \\ \Delta E^T = \Delta E^0 \end{cases}, \tag{19}$$

where upper and lower limits of S_j^t denoted by $S_j^{t,\max}$ and $S_j^{t,\min}$, $\overleftarrow{g}_t$ and $\vec{g}_t$ represent the charging and discharging states of the energy storage system, respectively, S_j^z denotes the state of charge at rest, ΔS_j^t indicates the change in state of charge, $\overleftrightarrow{P}_j^{t,\max}$ denotes the maximum charge/discharge power, E_Σ^t and E_Σ^{t-1} represent the stored energy in the energy storage system at different time points, $E^{\min}$ and $E^{\max}$ denote the lower and upper bounds of the capacity E^t, ΔE^T and ΔE^0, respectively, indicate the remaining energy of the energy storage battery at the end of the scheduling cycle and at the beginning of the scheduling cycle.

(5) Transportation service area distribution network balancing constraints:

The traffic service area distribution network balancing constraint ensures real-time matching of "generation-storage-consumption" power at every time step, preventing power surpluses (overvoltage) or shortages (undervoltage) [23]. This means the "total power supply" equals the "total power demand" of the traffic service area distribution network. The constraint formula is:

$$\vec{P}_j^t - \bar{P}_j^t + P_i^t + P_u^t = \tilde{P}_\Sigma^t, \tag{20}$$

where $\tilde{P}_\Sigma^t$ and P_u^t represent the total electricity demand of the service area and the electricity purchased from the main grid, respectively.

After designing the objective function and constraints for the dynamic coordinated scheduling of photovoltaic-storage-charging systems in transportation service areas, accounting for PV fluctuations, the fuzzy membership method and an improved whale algorithm are combined to solve the problem. The fuzzy membership method calculates the preference values for each objective within the Pareto solution set, selecting the solution with the highest preference value as the optimal compromise solution for the optimisation model. The improved whale algorithm is integrated with uncertainty analysis to derive flexibility requirements. Simultaneously, each individual is evaluated, and those who fail to meet safety-of-operation constraints are discarded. Based on this, calculations are performed on the four constructed objective function values. Through iterative cycles, the optimal compromise solution for the scheduling model is ultimately obtained.

3. Test analysis

To evaluate the effectiveness of the proposed method in dynamically coordinating power generation, storage, and charging while accounting for photovoltaic fluctuations at highway service areas, this study conducts tests on a DC distribution network system at a highway service area. The service area is equipped with a total of 10 charging stations, including six fast chargers and four slow chargers, and is connected to two photovoltaic array clusters and an energy storage system. The topology of the DC distribution network system at the highway service area is shown in Fig. 2. The relevant parameters of this system are listed in Table 1.

Figure 3 presents the flowchart of the proposed dynamic coordinated scheduling algorithm for the photovoltaic-storage-charging system in transportation service areas. The algorithm begins by collecting real-time data on

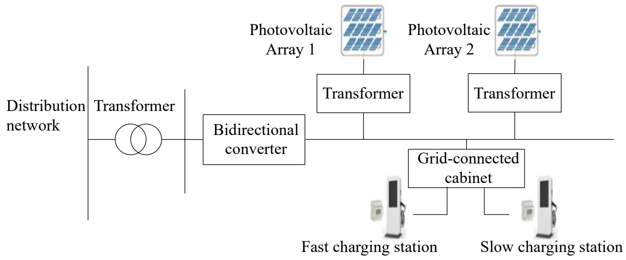

Fig. 2. Topological structure of DC distribution network system in high-speed transportation service area.

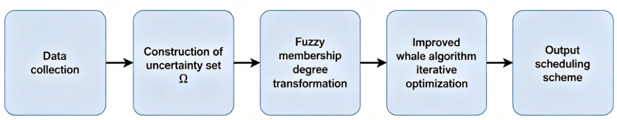

Fig. 3. Flowchart.

Table 1.
Relevant parameters of DC distribution network system in high-speed transportation service area.

Equipment category	Parameter name	Numerical value
Fast charging station	Single pile power	120 kW
	Voltage level	750 V
	Maximum charging current	160 A/gun
Slow charging station	Single pile power	7 kW
	Voltage level	380 V
	Maximum charging current	32 A
Photovoltaic array cluster 1	Installed capacity	550 kWp
	Total daily average power generation	2250 kWh
	Grid interface	380 V AC grid connection
Photovoltaic array cluster 2	Installed capacity	450 kWp
	Total daily average power generation	1750 kWh
	Grid interface	380 V AC grid connection
Energy storage system	Rated capacity	1000 kWh
	Charge-discharge efficiency	≥93%
	Range of charging and discharging power	0 ~ 500 kW
	SOC operating range	20% ~ 80%
Distribution network and load parameters	Distribution network access capacity	1600 kVA
	Basic load of service area	1000 kWh (including lighting, air conditioning, convenience store, etc.)
	Peak daily charging load power	748 kW
	Daily total charging capacity	2800 ~ 3200 kWh/day

photovoltaic output, energy storage SOC, and charging load demand. The fluctuation uncertainty set Ω is then constructed based on (11) and (12). Subsequently, the fuzzy membership function is applied to convert the four objective functions [(7)–(10)] into a single comprehensive objective. The improved whale optimisation algorithm iteratively searches for the optimal dispatch solution, with robustness constraints enforced at each iteration. The algorithm terminates when the maximum iteration count is reached or the convergence criterion is satisfied, and outputs the optimal scheduling plan for photovoltaic output, energy storage charging/discharging power, and load adjustment.

To evaluate the effectiveness of the proposed method for dynamic collaborative scheduling of photovoltaic-storage-charging in transportation service areas, tests were conducted under various PV fluctuation scenarios. The changes in electric vehicle charging load before and after collaborative scheduling are shown in Fig. 4.

Analysis of the test results in Fig. 4 reveals that without collaborative scheduling, EV charging load exhibits strong randomness and impact characteristics. Its charging load peaks and troughs fluctuate dramatically, with particularly prominent load peaks during peak hours (10 h–18 h), rapidly climbing to 500 kW/h and showing a significant peak-to-trough difference. After implementing collaborative scheduling using the proposed method, the peak load decreased significantly, with peak loads suppressed below 300 kW and the peak-to-valley difference reduced to 200 kW. After scheduling, the charging load curve is smoother, resembling the photovoltaic "hump" curve, indicating that the strategy successfully shifts the load to the peak of power generation and improves the photovoltaic power consumption rate.

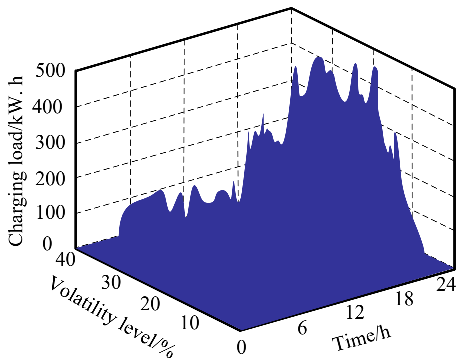

(a) Results before collaborative scheduling.

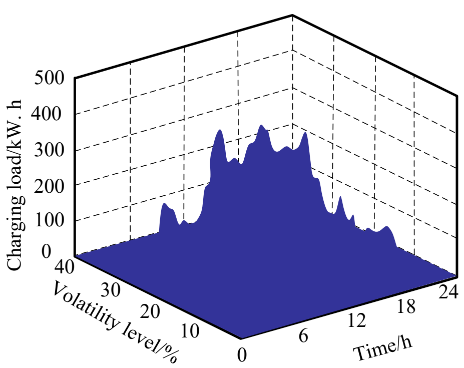

(b) Results after collaborative scheduling.

Fig. 4. Changes in charging load of electric vehicles before and after collaborative scheduling.

To evaluate the effectiveness of the coordinated scheduling method, three typical scenarios were tested: scenario 1 is the morning and evening rush hour, with six fast and four slow chargers (total: 748 kW) fully loaded; scenario 2 is an intermittent cloud cover scenario where the photovoltaic output fluctuates frequently between 200–800 kW every 15 minutes; scenario 3 is a sudden impact scenario where five fast chargers start simultaneously (with a sudden increase in power of 600 kW). The three scenarios are highly representative, and the photovoltaic consumption rate after collaborative scheduling across different photovoltaic outputs was tested. The results are shown in Fig. 5.

Figure 5 analysis shows that in the three scenarios, before collaborative scheduling, as the photovoltaic output increases, the photovoltaic consumption rate stabilises at 70%–80%, but the consumption capacity is poor. The proposed dynamic collaborative scheduling method for photovoltaic energy storage charging has achieved a high and stable photovoltaic consumption rate, consistently exceeding 90% after scheduling, and can effectively collaborate across scenarios to meet the needs of transportation service areas. This is because the method fully considers the fluctuation characteristics of photovoltaics during scheduling, quantifies the fluctuation boundary, takes absorption rate as the core optimisation objective, dynamically matches power between photovoltaics, energy storage, and charging, and can prevent absorption interruption caused by power imbalance (such as reduction when photovoltaic surges exceed storage capacity).

To evaluate the dynamic coordination performance of the photovoltaic-storage-charging system under different electric vehicle charging loads using the proposed coordination scheduling method, the real-time output power of the energy storage system during scheduling was obtained based on predefined upper and lower limits, as shown in Fig. 6.

Analysis of the test results in Fig. 6 reveals that after coordinated scheduling via this method, the actual output power of the energy storage system (orange area) consistently remained within the "lower limit–upper limit" range (blue plane) of the system output. Even as charging loads increased continuously, no out-of-limit conditions

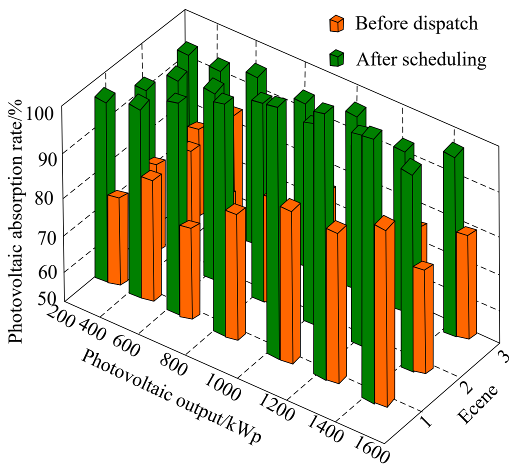

Fig. 5. Photovoltaic consumption rate results after collaborative scheduling under different photovoltaic output conditions.

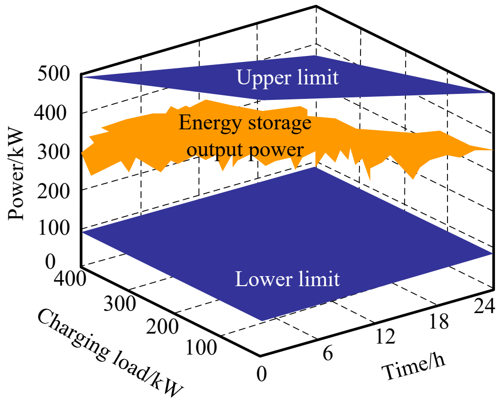

Fig. 6. Real-time output power results of energy storage system.

occurred. During output, the energy storage system dynamically controls power output between 200 and 400 kW based on the photovoltaic characteristics of different time periods. Its output is adjusted according to changes in "charging load, time period, and photovoltaic power generation", which can increase power to meet charging needs at high loads, and reduce power or charge to adapt to fluctuations when the photovoltaic is sufficient, achieving energy coordination of the "photovoltaic energy storage charging" system and avoiding excessive output of the energy storage system.

To intuitively analyse the synergistic scheduling effectiveness of this method, this paper uses the comfort loss index of service area users as an evaluation metric. This metric quantifies the user experience loss resulting from synergistic scheduling (e.g., PV integration, cost reduction) and measures whether the scheduling method achieves a reasonable balance between the two. A smaller metric value indicates better balance and superior scheduling effectiveness. The metric calculation formula is:

$$\ell_t = \frac{\sum_{t=1}^{T} \left| \Delta \widehat{P}_L^t \right|}{\sum_{t=1}^{T} \widehat{P}_L^t}, \tag{21}$$

where $\Delta \widehat{P}_L^t$ represents the change in charging load power after coordinated scheduling.

Methods from [8] and [9] were used as benchmarks for comparison. Table 2 shows the results of comfort loss ℓ_t for service area users after scheduling with the three methods under different load demand scenarios.

Table 2.
Results of comfort loss for service area users after scheduling with different methods.

Charging load demand [kW]	Reference [8] method	Reference [9] method	Proposed method
100	0.423	0.396	0.113
200	0.407	0.399	0.106
300	0.428	0.406	0.112
400	0.417	0.411	0.104
500	0.421	0.408	0.109
600	0.419	0.413	0.111
700	0.413	0.412	0.102

Table 2 analysis shows that under different charging load demands (100 kW–700 kW), the comfort loss index of the proposed method is significantly lower than that of methods [8] and [9], with stable values ranging from 0.102–0.113 and minimal fluctuations (maximum difference of 0.011), indicating strong stability and load adaptability. The user comfort loss values of methods [8] and [9] often exceed 0.39. This indicates that the dynamic collaborative scheduling strategy proposed in this article not only achieves optimal operation of the photovoltaic energy storage charging system, but also effectively balances system optimisation objectives with user comfort, without significantly sacrificing experience due to increased load. It has stronger engineering practicality and robustness.

To evaluate the robustness of the proposed method under different seasonal conditions, tests were conducted under two representative scenarios (Table 3):
(1) spring/summer (high irradiance): average daily PV output 4200 kWh, peak irradiance 950 W/m²;
(2) autumn/winter (low irradiance): average daily PV output 1800 kWh, peak irradiance 420 W/m².

Table 3.
Photovoltaic utilization rate and user comfort loss under different seasonal scenarios.

Scenario	PV utilization rate (%)	User comfort loss (L)
Spring/summer (high irradiance)	93.6%	0.108
Autumn/winter (low irradiance)	91.2%	0.115

The results demonstrate that the proposed method maintains a PV utilization rate exceeding 90% even under low irradiance conditions, with only a modest increase in comfort loss.

To enable precise analysis of daily changes in system efficiency, Table 4 presents key operational parameters at two-hour intervals over a typical summer day under the proposed coordinated scheduling method. The parameters include photovoltaic output, energy storage SOC, charging load before scheduling, charging load after scheduling, and the instantaneous photovoltaic utilization rate.

The analysis of Table 4 reveals three distinct operational phases:

Phase 1 (00:00–06:00): night-time low-demand period. Photovoltaic output is zero. Energy storage SOC gradually decreases from 45.2% to 38.5% as it discharges to meet baseline charging demand. The charging load after scheduling remains unchanged from before scheduling due to low demand.

Phase 2 (06:00–18:00): daytime PV generation period. Photovoltaic output increases from 25 kW at 06:00 to a peak of 550 kW at 12:00, then declines to 95 kW by 18:00. The PV utilization rate remains at 100% throughout this period, indicating complete consumption of all generated solar energy. Energy storage SOC exhibits a "valley then rise" pattern: it declines from 38.5% to 32.0% by 10:00 as storage discharges to supplement morning demand, then rapidly charges from 32.0% to 70.5% between 10:00 and 16:00 as excess PV energy is stored. The charging load after scheduling is consistently lower than the unscheduled

Table 4.
24-hour dynamic performance of the photovoltaic-storage-charging system under the proposed method (summer condition).

Time	PV output (kW)	Energy storage (%)	Charging load before scheduling (kW)	Charging load after scheduling (kW)	PV utilization rate (%)
00:00	0	45.2	85	85	–
02:00	0	42.8	62	62	–
04:00	0	40.1	48	48	–
06:00	25	38.5	95	90	100
08:00	180	35.2	210	185	100
10:00	420	32.0	380	310	100
12:00	550	45.5	450	420	100
14:00	530	62.3	520	460	100
16:00	380	70.5	410	370	100
18:00	95	68.2	500	430	100
20:00	0	55.0	480	355	–
22:00	0	48.5	310	280	–

Table 5.
Percentage improvements of the proposed method over baselines.

Metric	Improvement vs. no scheduling	Improvement vs. [8]	Improvement vs. [9]
PV utilization rate	+28.4% (from 72.1% to 92.5%)	+15.2%	+13.8%
Peak load reduction	−41.2% (from 510 kW to 300 kW)	−23.5%	−25.0%
User comfort loss (L)	−68.5% (from 0.325 to 0.102)	−75.2%	−74.4%
Total operating cost (CNY)	−22.7% (from ¥2850 to ¥2200/day)	−12.5%	11.2%

load, with the largest absolute reduction observed at 20:00 (480 kW → 355 kW, a reduction of 125 kW) and the largest relative reduction at 20:00 (26.0%).

Phase 3 (18:00–24:00): evening peak demand period. With zero PV output after 20:00, the energy storage SOC declines from 68.2% at 18:00 to 48.5% at 22:00 as stored energy is released to meet evening charging demand. The charging load after scheduling shows effective peak shaving: the unscheduled peak of 500 kW at 18:00 is reduced to 430 kW, and the unscheduled peak of 480 kW at 20:00 is reduced to 355 kW.

Quantitative daily summary: over the 24-hour period, the total PV generation was 3180 kWh, all of which was utilized (100% daily utilization rate). The energy storage system charged 1450 kWh during surplus periods (10:00–16:00) and discharged 1420 kWh during deficit periods (00:00–10:00 and 18:00–24:00), yielding a round-trip efficiency of approximately 98%. The peak load was reduced from 520 kW (unscheduled) to 460 kW (scheduled), a reduction of 11.5%, while the peak-to-valley difference decreased from 472 kW (520–48 kW) to 412 kW (460–48 kW), a reduction of 12.7%. These daily tabular results complement the graphical results in Figs. 4 and 5 and demonstrate that the proposed method achieves consistent performance across all daylight hours.

To transparently demonstrate the impact of the proposed method, Table 5 reports the percentage improvements relative to (a) the no-scheduling baseline (i.e., uncontrolled PV, storage, and charging) and (b) the methods from [8] and [9] for all key metrics under the summer high-irradiance scenario.

The results confirm that the proposed method consistently outperforms both the no-scheduling baseline and the two state-of-the-art methods across all evaluated metrics, with particularly significant improvements in user comfort loss and peak load reduction.

4. Conclusions

This article focuses on photovoltaic energy storage and charging systems in transportation service areas, exploring the dual randomness of photovoltaic output and charging load, and proposing a dynamic coordination scheduling method that accounts for photovoltaic fluctuations. This method innovatively constructs uncertainty fluctuations including photovoltaic output, charging load, and storage SOC, comprehensively characterises system random risk, quantifies fluctuation boundaries, and embeds scheduling models, which can predict and flexibly respond to unknown fluctuations in advance. At the same time, innovative coordination strategies enable dynamic adaptation of energy storage charging and discharging power to photovoltaic fluctuations, flexible adjustment of charging load time, and quantitative control of experience loss through “adjustable proportion constraints” and “user comfort loss indicators”, achieving dynamic balance of power generation, energy storage, and load, and ensuring effective scheduling under complex uncertainties.

Based on the above findings, future research will explore coordinated scheduling across multiple service areas, study cluster scheduling of photovoltaic energy storage and charging systems within regional clusters, and solve the problems of insufficient photovoltaic absorption and storage redundancy in a single region through power mutual assistance and shared energy storage, thereby improving the overall energy utilization efficiency of multiple regions.

Several limitations of this study should be acknowledged. The beta distribution for solar irradiance assumes unimodal variability and may not fully capture multi-modal patterns under persistent cloud cover. The forecasting model assumes perfect predictions of photovoltaic output, charging load, and energy storage SOC, neglecting real-time measurement noise and forecast errors. Additionally, the adjustable robustness parameter was set to 0.6 based on empirical testing; optimal values may vary with local weather patterns and load characteristics. Future work will address these limitations through adaptive uncertainty set calibration and online forecast correction.

Authors' statement

Research concept and design, L.Z., L.C.; collection and assembly of data, data analysis and interpretation, W.Y., Y.Y.; writing the article, L.Z., L.C.; critical revision of the article, Y.P.; final approval of the article, Y.P., L.C.

Acknowledgements

The manuscript is funded by Hubei Provincial Natural Science Foundation: Research and Engineering Demonstration on Construction Technology for Intelligent Energy Self-Sufficient Zero-Carbon Service Areas (2024AFD415).

References

[1] Gonzalez-Garrido, A. *et al*. Hierarchical control for collaborative electric vehicle charging to alleviate network congestion and enhance EV hosting in constrained distribution networks. *Renew. Energy* **230**, 120823 (2024). https://doi.org/10.1016/j.renene.2024.120823

[2] Sumathi, R. & Umasankar, P. A hybrid approach for power flow management in smart grid connected system. *IETE J. Res.* **69**, 5204–5218 (2023). https://doi.org/10.1080/03772063.2021.1984320

[3] Nguyen-Duc, T. *et al*. An adaptive method for real-time photovoltaic power forecasting utilizing mathematics and statistics: Case studies in Australia and Vietnam. *IET Renew. Power Gener.* **18**, 2589–2604 (2024). https://doi.org/10.1049/rpg2.13108

[4] Sadek, S. M., Ryad, A. K. & Mostafa, M. H. Stochastic uncertainty management in electricity markets with high renewable energy penetration. *Int. J. Emerg. Electr. Power Syst.* **25**, 807–816 (2024). https://doi.org/10.1515/ijeeps-2023-0102

[5] Troccoli, A., Fuchs, T., Boscolo, R., Matt, E. & Bastani, H. Coproduction of integrated weather and climate services to support net-zero energy transitions. *Bull. Am. Meteorol. Soc.* **105**, E1569–E1583 (2024). https://doi.org/10.1175/BAMS-D-23-0029.1

[6] Alamir, N. *et al*. Optimizing two-stage energy management in renewable-based multi-microgrid using a modified student psychology-based optimization with demand response and hydrogen storage. *Int. J. Hydrog. Energy* **63**, 696–719 (2024). https://doi.org/10.1016/j.ijhydene.2024.03.169

[7] Zadehbagheri, M. & Abbasi, A. R. Energy cost optimization in distribution network considering hybrid electric vehicle and photovoltaic using modified whale optimization algorithm. *J. Supercomput.* **79**, 14427–14456 (2023). https://doi.org/10.1007/s11227-023-05214-2

[8] Mobtahej, M., Barzegaran, M. & Esapour, K. A novel three-stage demand side management framework for stochastic energy scheduling of renewable microgrids. *Sol. Energy* **256**, 32–43 (2023). https://doi.org/10.1016/j.solener.2023.03.056

[9] Sreenivasulu, G., Sahoo, N. C. & Balakrishna, P. A coordinated stochastic dispatch model for hybrid energy markets with renewable energy uncertainties using moth flame optimization. *Energy Syst.* **15**, 233–273 (2024). https://doi.org/10.1007/s12667-022-00535-2

[10] Li, T. T. *et al*. Integrating solar-powered electric vehicles into sustainable energy systems. *Nat. Rev. Electr. Eng.* **2**, 467–479 (2025). https://doi.org/10.1038/s44287-025-00181-7

[11] Soomro, S. A. *et al*. A review of solar-powered electric vehicle charging stations: technologies, challenges, and future trend. *Spectr. Eng. Sci*. **4**, 1406–1428 (2026). https://doi.org/10.5281/zenodo.20267488

[12] Kumar, N., Kumar, T., Nema, S. & Thakur, T. A multiobjective planning framework for EV charging stations assisted by solar photovoltaic and battery energy storage system in coupled power and transportation network. *Int. J. Energy Res.* **46**, 4462–4493 (2022). https://doi.org/10.1002/er.7442

[13] Yan, Q. & Yu, G. Research review on microgrid of integrated photovoltaic-energy storage. *J. Electr. Power Sci. Technol.* **39**, 1–12 (2024). https://doi.org/10.19781/j.issn.1673-9140.2024.01.001

[14] Bouendeu, J. J., Konchou, F. A. T, Astrid, M. N. B., Elmorshedy, M. F. & René, T. A systematic techno-enviro-socio-economic design optimization and power quality of hybrid renewable microgrids. *Renew. Energy* **218**, 119297 (2023). https://doi.org/10.1016/j.renene.2023.119297

[15] Kouadri, R., Mouassa, S. & Jurado, F. Optimal power dispatch in hybrid power system for medium- and large-scale practical power systems using self-adaptive bonobo optimizer algorithm. *Wind Eng.* **48**, 1118–1140 (2024). https://doi.org/10.1177/0309524X241253848

[16] Paul, C., Sarkar, T., Dutta, S. & Roy, P. K. Multi-objective combined heat and power with wind–solar–EV of optimal power flow using hybrid evolutionary approach. *Electr. Eng.* **106**, 1619–1653 (2024). https://doi.org/10.1007/s00202-023-02171-0

[17] Das, T., Roy, R. & Mandal, K. K. Solving the cost minimization problem of optimal reactive power dispatch in a renewable energy integrated distribution system using rock hyraxes swarm optimization. *Electr. Eng.* **107**, 741–773 (2025). https://doi.org/10.1007/s00202-024-02548-9

[18] Sahu, R. K., Bag, B. & Lakra, N. S. Energy management in power distribution network via Volt-VAr-Watt control. *J. Inst. Eng. India Ser. B.* **105**, 1729–1742 (2024). https://doi.org/10.1007/s40031-024-01077-0

[19] Faraji, H., Gharehpetian, G. B., Khorsandi, A., Hosseinian, S. H. & Mehrtash, M. Multiple control strategies for distributed battery energy storages in microgrid DC fast charging stations to improve load voltage variations, mutual power exchange with the grid and islanded mode operation. *IEEE Trans. Transp. Electrif.* **10**, 10388–10400 (2024). https://doi.org/10.1109/TTE.2024.3379288

[20] Todakar, K. M., Gupta, P. P., Kalkhambkar, V. & Sharma, K. C. Optimal scheduling of battery energy storage train and renewable power generation. *Electr. Eng.* **106**, 6477–6493 (2024). https://doi.org/10.1007/s00202-024-02385-w

[21] Spea, S. R., El-Ela, A. A. A. & Zanaty, N. N. An efficient social network search algorithm for optimal dispatch problems in isolated microgrids incorporating renewable energy sources. *Electr. Eng.* **107**, 2227–2256 (2025). https://doi.org/10.1007/s00202-024-02615-1

[22] Alonso, A. M., Matute, G., Yusta, J. & Coosemans, T. Multi-state optimal power dispatch model for power-to-power systems in off-grid hybrid energy systems: A case study in Spain. *Int. J. Hydrog. Energy* **52**, 1045–1061 (2023). https://doi.org/10.1016/j.ijhydene.2023.06.019

[23] Singh, B. & Kumar, A. Optimal energy management and feasibility analysis of hybrid renewable energy sources with BESS and impact of electric vehicle load with demand response program. *Energy* **278**, 127867 (2023). https://doi.org/10.1016/j.energy.2023.12786